Mycobacterium tuberculosis Expresses a Novel pH-dependent Divalent Cation Transporter Belonging to the Nramp Family

By Daniel Agranoff,* Irene M. Monahan,‡ Joseph A. Mangan,‡ Philip D. Butcher,‡ and Sanjeev Krishna*

*From the *Department of Infectious Diseases and the ‡Department of Medical Microbiology, St. George's Hospital Medical School, London SW17 ORE, United Kingdom*

Summary

Mammalian natural resistance–associated macrophage protein (Nramp) homologues are important determinants of susceptibility to infection by diverse intracellular pathogens including mycobacteria. Eukaryotic Nramp homologues transport divalent cations such as Fe^{2+}, Mn^{2+}, Zn^{2+}, and Cu^{2+}. *Mycobacterium tuberculosis* and *Mycobacterium bovis* (bacillus Calmette-Guérin [BCG]) also encode an Nramp homologue (Mramp).

RNA encoding Mramp induces ~20-fold increases in $^{65}Zn^{2+}$ and $^{55}Fe^{2+}$ uptake when injected into *Xenopus laevis* oocytes. Transport is dependent on acidic extracellular pH and is maximal between pH 5.5 and 6.5. Mramp-mediated $^{65}Zn^{2+}$ and $^{55}Fe^{2+}$ transport is abolished by an excess of Mn^{2+} and Cu^{2+}, confirming that Mramp interacts with a broad range of divalent transition metal cations.

Using semiquantitative reverse transcription PCR, we show that *Mramp* mRNA levels in *M. tuberculosis* are upregulated in response to increases in ambient Fe^{2+} and Cu^{2+} between <1 and 5 μM concentrations and that this upregulation occurs in parallel with mRNA for y39, a putative metal-transporting P-type ATPase. Using a quantitative ratiometric PCR technique, we demonstrate a fourfold decrease in *Mramp/y39* mRNA ratios from organisms grown in 5–70 μM Cu^{2+}. *M. bovis* BCG cultured axenically and within THP-1 cells also expresses mRNA encoding Mramp.

Mramp exemplifies a novel prokaryotic class of metal ion transporter. Within phagosomes, Mramp and Nramp1 may compete for the same divalent cations, with implications for intracellular survival of mycobacteria.

Key words: bacillus Calmette-Guérin • *Xenopus* oocyte • metal ion • phagosome • intracellular pathogen

The macrophage vacuole is an especially hostile microenvironment for intracellular pathogens, as it is the arena in which multiple host defences operate. Many phylogenetically unrelated pathogens, including *Mycobacteria*, *Salmonella*, and *Leishmania* species, have successfully adapted to this niche (1, 2). A critical determinant of susceptibility to infection by these organisms is the natural resistance–associated macrophage protein (Nramp)[1] family (3). Nramp homologues are phylogenetically ancient integral membrane proteins first identified in mice (4). A mutation in *Nramp1* (originally designated *Bcg/Lsh/Ity*) renders mice susceptible to uncontrolled proliferation of many organisms (*Mycobacterium bovis* [BCG], *Mycobacterium avium*, *Mycobacterium lepraemurium*, *Leishmania donovani*, and *Salmonella typhimurium*) within the reticuloendothelial system during the early phase of infection (5–7). Genetic analyses have now linked polymorphisms in and around the *Nramp1* locus with susceptibility to tuberculosis (8) and leprosy (9) in humans.

Nramp homologues in yeast (10) and rats (11, 12) transport cations such as Fe^{2+}, Cu^{2+}, and Zn^{2+}, and deficient Mn^{2+} uptake is implicated in *Drosophila* mutants without a functional Nramp homologue (13). These cation substrates of Nramp are important in monocytes, neutrophils, and macrophages because they are involved in generating reactive oxygen intermediates during the respiratory burst. For example, hydrogen peroxide generated by the respiratory burst interacts with Fe^{2+}/Fe^{3+}, and produces reactive hydroxyl and superoxide radicals that are crucial in early defence against intracellular microorganisms. Consistent with this function, Nramp1 (a mammalian homologue) expres-

[1]*Abbreviations used in this paper:* BCG, bacillus Calmette-Guérin; 2-DOG, 2′-deoxy-[^{14}C]d-glucose; Mramp, mycobacterial homologue of Nramp; Nramp, natural resistance–associated macrophage protein; ORF, open reading frame; RT, reverse transcription; SUM, standard uptake medium; TC, tandem competitive.

sion is restricted to phagosomes of myelocytic cells (14). Some transition metals are also components of bacterial metalloenzymes (such as the superoxide dismutases and catalases) that protect bacteria against oxidative stresses encountered, for example, in phagosomes (15, 16).

We (17) and others (18, 19) have hypothesized that both mycobacteria and macrophages use Nramp homologues to compete for intraphagosomal metal ions. We now provide evidence that Mramp (the mycobacterial homologue of Nramp) is a pH-dependent divalent cation transporter of broad specificity. Mramp expression is modulated by variation in ambient Cu^{2+} and Fe^{2+} concentrations as well as being expressed in intracellular mycobacteria.

Materials and Methods

Isolation and Cloning of Mramp Sequence. We used the previously identified *M. leprae* sequence encoding an Nramp homologue to search the EMBL database using TBLASTN (20). PCR on genomic DNA from *M. tuberculosis* (H37Rv) and BCG using Pfu polymerase (Stratagene, Inc.) was carried out with primers designed to introduce BglII restriction sites and a strong eukaryotic Kozak consensus (TTGGTGG to ATGATGG, initiation codon underlined). PCR primers were as follows: 5′-GTA GCC AGA TCT ATG **ATG** GCG GGC GAA TTT CGG-3′ and 5′-GCG GTC AGA TCT TCA GCC GGT CAC CGT GAG ATA-3′ (BglII sites are underlined and the translational start codon is in bold). Cycle conditions were as follows: 1 min at 94°C, 35 cycles of 30 s at 94°C, 30 s at 66°C, 2 min at 72°C, with a final 4-min hold at 72°C. The reaction was supplemented with Mg^{2+} (1 mM) and Betaine (1 M) (Sigma Chemical Co.). The PCR product from *M. tuberculosis* was subcloned into BglII sites in pSP, which contains 5′ and 3′ untranslated *Xenopus* β-globin sequences (21) and was verified by sequence analysis. Constructs containing both orientations of *Mramp* were obtained and designated pXmramp (sense) and pXpmarm (antisense).

Expression of Mramp in Xenopus Oocytes and Fe^{2+} and Zn^{2+} Uptake Studies. *Xenopus laevis* oocytes were prepared as described previously (22). Capped cRNA encoding Mramp was transcribed (MEGAscript™ SP6; Ambion) from Xba1-linearized templates (pXmramp and pXpmarm), and oocytes were injected with cRNA (5 ng in 50 nl of water) or a corresponding volume of RNAse-free water. Fe^{2+} and Zn^{2+} uptake assays were performed after 48–96 h incubation in Barth's solution (88 mM NaCl, 1 mM KCl, 2.4 mM $NaHCO_3$, 15 mM Hepes [pH 7.6], 0.3 mM $Ca(NO_3)_2.4H_2O$, 0.41 mM $CaCl_2.6H_2O$, 0.82 mM $MgCl_2.7H_2O$, 10 μg/ml penicillin, 10 μg/ml streptomycin) at 19°C (23).

$^{65}Zn^{2+}$ uptake assays were performed on batches of 10–15 oocytes washed 4 times in freshly made up standard uptake medium (SUM: 90 mM KCl, 10 mM NaCl, 10 mM morpholinoethane sulfonic acid [MES], pH 5.0–pH 6.5; as before but with 10 mM Hepes at pH 7.0) and incubated in SUM for 1–4 h at room temperature with 100 μM $^{65}ZnCl_2$ (Nycomed Amersham plc). Transport was terminated by washing oocytes in excess ice-cold SUM. $^{65}Zn^{2+}$ uptake was quantitated in individual oocytes on a Wallac Wizard 1480 gamma counter and corrected for uptake into water or antisense cRNA–injected controls.

$^{55}Fe^{2+}$ uptakes were performed with $^{55}Fe^{2+}$ (5 μM in 100 μM total Fe^{2+}; Nycomed Amersham plc) in SUM containing ascorbic acid (2 mM) to maintain iron in a ferrous state, and all studies used fresh solutions to minimize reoxidation of Fe^{2+}. The amount of ferrous iron was verified by a ferrozine assay (24). Quantitation of ^{55}Fe uptake was by scintillation counting (Wallac Microbeta Plus).

Maximal expression of both $^{65}Zn^{2+}$ and Fe^{2+} uptake occurred between 2 and 4 d after microinjection. Competitions with divalent cations were performed using $^{65}Zn^{2+}$ or Fe^{2+} as permeants and 100-fold excess (10 mM) concentrations of $CuCl_2$, $MnCl_2$, $FeCl_2$, $ZnCl_2$, and $MgCl_2$.

Media for M. tuberculosis Cultures. All glassware was autoclaved after rinsing in 0.2 N HCl followed by deionized water to remove trace quantities of iron. Low Fe (~5 μM) Sauton's medium for starter cultures consisted of asparagine (15 mM), $MgSO_4$ (1 mM), sodium citrate (4 mM), KH_2PO_4 (7 mM), and glycerol (2% vol/vol, pH 7.1). Fe-depleted Sauton's medium (<1 μM) was prepared as above, omitting $MgSO_4$, and stirred overnight at 4°C with Chelex 100 (10 g/l). After filter sterilization, the medium was supplemented ($MgSO_4$ [1 mg/ml equivalent to 8.3 mM final concentration], $ZnSO_4.4H_2O$ [0.2 μg/l final concentration ~ 1 nM], and $MnCl_2.4H_2O$ [0.2 μg/l ~ 1 nM]) to compensate for losses during chelation. Media containing "low Fe" (<1 μM), "medium Fe" (4 μM), or "high Fe" (48 μM) and "low Cu" (<0.5 μM), "medium Cu" (5 μM), or "high Cu" (69.8 μM) were prepared by additionally supplementing aliquots of this medium with ferric ammonium citrate (~16% Fe content) or $CuCl_2$. To ensure that concentrations of cations not being studied were above limiting concentrations, the Fe-modified media were supplemented with Cu (~1 μM), and Cu-modified media with Fe (4 μM). Concentrations of Fe and Cu in these media were verified by ferrozine assay (24) and atomic absorption spectrophotometry, respectively. All chemicals were obtained from Sigma-Aldrich.

Growth of M. tuberculosis in Varying Iron and Copper Concentrations. Starter cultures in Dubos broth supplemented with 10% Dubos medium albumin (Difco) were initiated from glycerol stocks and grown at 37°C to mid-log phase. These were inoculated (1:10) into low iron Sauton's medium, grown for 1 wk (37°C, 5% CO_2, without shaking), and subcultured to ensure complete depletion of iron and copper. 10 ml of these cultures was inoculated into Fe/Cu-depleted Sauton's medium (10 ml into 190 ml) supplemented to give low, medium, or high concentrations of iron or copper and grown for 5 wk.

Infection of Macrophages with BCG. As BCG encodes an Mramp sequence (available from EMBL/GenBank/DDBJ under accession no. AJ005699) identical to that of *M. tuberculosis*, we used BCG as a model to examine the expression of Mramp during intracellular infection. The human macrophage cell line, THP-1, was maintained as suspended cells and passaged at a density of 2–5 × 10^6 cells/ml. Before infection with BCG, the cells were passaged at least three times in antibiotic-free RPMI 1640 (ICN Biochemicals) supplemented with heat-inactivated FCS (10%), grown to a density of 2–5 × 10^6 cells/ml, and stimulated with PMA (20 mM; Sigma Chemical Co.) for 24 h to induce adherence. Nonadherent cells were removed by washing twice in PBS, and the resulting monolayers (~3–5 × 10^7 cells/flask) were covered with supplemented RPMI 1640. Mid-log phase bacteria were pelleted from Dubos broth (500 *g*, 10 min), resuspended in medium, and sonicated (Rinco Ultrasonics) for 15 s (five 3-s bursts at 70% amplitude) to disaggregate bacterial clumps. The sonicate was added to macrophages (10 bacilli/macrophage) and left for 24 h (37°C, 5% CO_2). Extracellular mycobacteria were removed by decanting the supernatant and extensively washing the adherent cells twice in PBS. Efficiency of phagocytosis was estimated to be ~30% by counting CFU in the collected wash-

ings and microscopic examination of Ziehl-Nielsen–stained macrophages. Macrophage viability (>90%) throughout these experiments was assessed by Trypan blue exclusion, with further details given in reference 25.

Recovery of RNA from Intracellular BCG. After extensive washing of the macrophage monolayer, mycobacteria were recovered from differentially lysed THP-1 cells by the addition of 20 ml GTC solution (4 M guanidinium thiocyanate [GTC; Fluka] containing 0.5% sodium *N*-lauroylsarcosine, 25 mM sodium citrate, pH 7, and 0.1 M 2-ME) to each flask (25). Total RNA was then extracted from the washed bacterial pellets as described previously (26).

Identification of Open Reading Frames. First strand cDNA synthesis on total RNA used random hexamer primers (Promega) and Moloney murine leukemia virus reverse transcriptase (Superscript II™; GIBCO BRL) according to the manufacturer's instructions. Contamination of RNA by genomic DNA was excluded by PCR on RNA template made without reverse transcriptase and on template made from RNA pretreated with RNAse A (Qiagen).

PCR was carried out using primers spanning the junction between the 3′ end of the *Mramp* gene and the open reading frame (ORF) immediately downstream under the following cycling conditions: 30 cycles of 1 min at 94°C, 2 min at 55°C, 3 min at 72°C. Primers were 5′-ACGATCACCCATAACAACAGG-3′ and 5′-CAGAGAACGACTTCACCAACC-3′.

Generation of Competitor for Tandem Competitive PCR. Templates for quantitative PCR assays were generated by oligonucleotide restriction site mutagenesis (27), using *M. tuberculosis* genomic DNA as template, and corresponded to the following fragments: for *Mramp* (467 bp, 820–1287), and for two "P"-type ATPases: *yhho* (503 bp, 79–582) and *y39* (503 bp, 100–603). Spanning primer pairs were as follows: for *Mramp*, 5′-CTGGTTGCCGCGCTGAACATG-3′ and 5′-GAACTGAAACCCCATTCAGCCGGTCACCGT-3′; for *y39*, 5′-GTTGGGGCCTCGAAGGAATTCGTTGACGCCGCA-3′ and 5′-CTTGCTGAACCACGCCAGCTT-3′; for *yhho*, 5′-ACCGGCTGAATGGGGTTTCAGTTCGACGCGGG-3′ and 5′-AACGAATTCCTTCGAGGCCCCAACCGCCAGCGC-3′.

Primers were designed so that the *Mramp* antisense primer overlapped with the *yhho* sense primer, and the *yhho* antisense primer overlapped with the *y39* sense primer, giving a tandemly organized construct after synthesis by PCR (28). PCR cycle conditions, identical for each fragment, were as follows: 3 min at 94°C, 35 cycles of 30 s at 94°C, 30 s at 65°C, 2 min at 72°C, followed by a 4-min hold at 72°C. To discriminate competitor from target in tandem competitive (TC)-PCR reactions, a mutant asymmetrical Kpn1 restriction site was introduced ~200 bp internal to the 5′ end of each fragment. These fragments were cloned in tandem into pGEM-T Easy (Promega). We chose "P"-type ATPase sequences (*y39*, putative Ca^{2+} transporter; and *yhho*, atypical heavy metal transporter reviewed in Agranoff et al. [17]) in order to quantitate the relative amounts of *Mramp* expression in mRNA obtained from mycobacteria cultured in different ionic microenvironments.

As an internal control for RNA preparations, we amplified 16S ribosomal RNA sequence using the primers 5′-CCC TTG TCT CAT GTT GCC AG and 5′-CTG GCA ACA TGA GAC AAG GG.

Quantitation of mRNA for Mramp and P-type ATPases. First strand cDNA synthesis on total RNA was carried out as described above. Semiquantitative estimates of mRNA expression were derived by conventional reverse transcription (RT)-PCR carried out under identical conditions for each primer pair and identical starting cDNA concentrations for all three genes. Products were quantified using a GDS 7600 system (Ultraviolet Products) and normalized to the most abundant product for each gene. Precise quantitation of relative amounts of cDNA for *Mramp* and *y39* under different growth conditions was carried out by TC-PCR. A series of PCR amplifications of each gene was carried out on a template mixture consisting of a fixed quantity of cDNA and serial dilutions (at 1/4 log intervals) of competitor molecule (linearized by Sac1 digestion). Products derived from competitor template could be distinguished from target product by KpnI digestion and were quantified as above. The plasmid competitor/cDNA ratio was calculated for individual reactions after heteroduplex correction and analyzed as published previously (29).

Statistical Analysis. Comparison of radioisotope uptake rates between two conditions was by the Mann Whitney U test, and comparison of uptakes at different pH values and with competitors was after Box-Cox transformation (to normalize distributions) and used MANOVA (v5.2 SYSTAT).

Results

Sequence Analysis of Mramp. A single *Nramp* homologue (designated *Mramp*) is located on cosmid MTY21C12 (GenBank/EMBL/DDBJ accession no. Z95210; gene number Rv0924c) in a 5286-bp region containing 5 ORFs oriented in the same direction (30). A potential ribosome binding site is immediately upstream of the first ORF with *Mramp* as the fourth gene in this series. To ascertain if *Mramp* is cotranscribed with neighboring ORFs, we carried out RT-PCR on total RNA extracted from cultured H37Rv using primers spanning the junction between the 3′ end of *Mramp* and the next ORF. A product of expected size (407 bp) was obtained (data not shown), indicating that *Mramp* is transcribed at least as a bicistronic operon. Database searches failed to identify functionally characterized homologues of this second ORF.

Mramp encodes a predicted 428–amino acid protein with a molecular mass of 44.9 kD and 10 transmembrane segments consistent with proposed topologies for yeast homologues (*smf1* and *2*) (31; Fig. 1). Compared with eukaryotic homologues, the hydrophilic NH_2-terminal region of Mramp, like those of other prokaryotic Nramp homologues, is shorter but exhibits a similar clustering of polar residues (31). The COOH terminus is also shorter and probably lacks the two final transmembrane segments predicted in some eukaryotic homologues. The amphiphilic properties of transmembrane segments M3, M5, and M9, in which the polar and nonpolar residues are segregated to opposite faces of the predicted α-helices (possibly forming a transmembrane channel), are also found in Mramp.

Sequence analysis of Mramp confirms that certain amino acid residues are highly conserved between all members of the Nramp family (Fig. 1). *Mramp* sequences from *M. tuberculosis* and BCG are identical and are most closely related to other bacterial homologues (72.4, 40, and 40% sequence identities with *M. leprae*, *Bacillus subtilis*, and *Escherichia coli*, respectively), whereas comparison with eukaryotic homologues gives overall amino acid identities of 21–24%. There

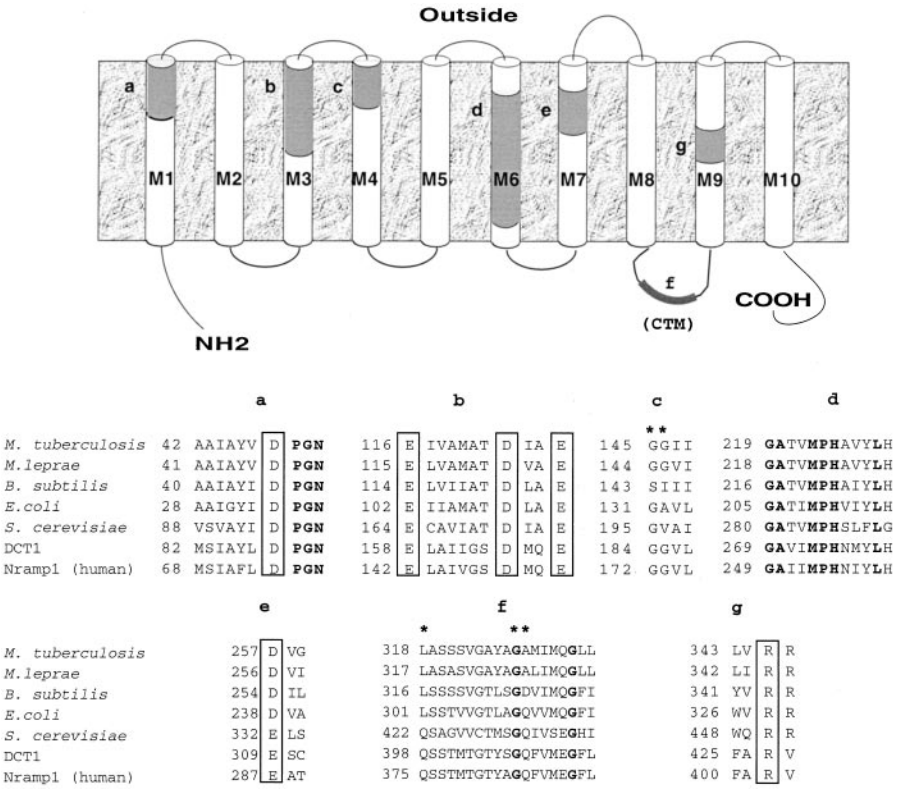

Figure 1. Putative distribution of membrane-spanning segments of Mramp to illustrate alignment of conserved residues with homologues. This sketch has been derived from detailed hydropathy analyses performed by Cellier et al. (reference 31). The precise number of membrane-spanning segments and topology of the COOH-terminal region are still uncertain. Mramp sequence was analyzed using the Kyte-Doolittle algorithm (window size of 16 amino acids). The highly conserved distribution of thermodynamically unfavored charged residues within transmembrane segments (M), which is a feature of eukaryotic Nramp homologues (reference 31), is also discernible in Mramp and other prokaryotic homologues (boxed residues). The positions of two adjacent glycine residues in M4 (region c, marked *) are known to be functionally important; in murine Nramp1, a G169D mutation is associated with the pathogen-susceptible phenotype (reference 3), while in Nramp2, a mutated neighboring glycine in the *mk* mouse (G185R; reference 36) and Belgrade (*b*) rat (reference 11) causes microcytic (iron deficiency) anemia, probably through steric and charge effects. Mramp contains a consensus transport motif (CTM) resembling the "EAA" box or "binding protein–dependent transport system's inner membrane component signature" (region f) (see reference 31). This motif [E,Q] [S,T,A]×2, 3X,G, [L,I,V,M,F,Y,A], 4X, [F,L,I,V], [P,K] is found in numerous bacterial periplasmic permeases and some eukaryotic multisubunit transporters (reference 31). Mutational analysis of three residues in this region (marked * in region f) in murine Nramp2 has demonstrated the functional importance of the first two residues (reference 10). Other highly conserved residues are shown in bold. DCT1 sequence = rat Nramp2; *S. cerevisiae* sequence = smf1. Sequence data are available from EMBL/GenBank/DDBJ under accession nos. U15184 (*M. leprae*), Z99106 (*B. subtilis*), U00096 (*E. coli*), U15929 (Smf1), AF008439 (DCT1), and L32185 (Nramp1, human).

is an asymmetrical distribution of charged amino acid residues between the endo- and exofacial regions of Mramp. This is consistent with similar patterns of charge distribution observed in many integral membrane proteins (32).

Mramp Induces $^{65}Zn^{2+}$ Uptake in Oocytes. Initially we cloned *Mramp* into pGEM-T Easy after mutating the mycobacterial GTG start codon to ATG without strengthening the Kozak consensus sequence. Microinjection of oocytes with RNA made from this construct induced up to twofold increases in $^{55}Fe^{2+}$ and $^{65}Zn^{2+}$ uptake compared with water-injected oocytes (data not shown). To optimize Mramp expression in oocytes, we retained the modified start codon, introduced a strong Kozak consensus, and cloned *Mramp* into a vector containing flanking *X. laevis* 5′ and 3′ untranslated regions (see Materials and Methods).

In 10 independent experiments, RNA derived from this latter construct induced large increases (up to 22-fold) in the accumulation of $^{65}Zn^{2+}$ by Mramp-expressing oocytes

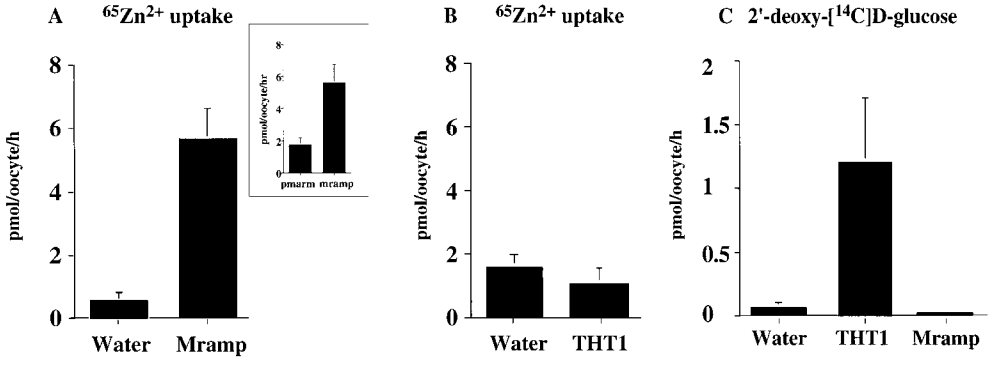

Figure 2. $^{65}Zn^{2+}$ uptake by oocytes expressing Mramp. (A) Induction of $^{65}Zn^{2+}$ uptake by Mramp in *Xenopus* oocytes injected with RNA (5 ng in 50 nl) transcribed from pXmramp. The difference in $^{65}Zn^{2+}$ uptake between experimental and water (50 nl)–injected control oocytes is highly significant ($P < 0.001$). Inset shows a separate experiment in which $^{65}Zn^{2+}$ uptake in Mramp cRNA–injected oocytes was compared with antisense cRNA (pmarm)-injected control oocytes ($P = 0.025$). (B) $^{65}Zn^{2+}$ uptake in water-injected and THT1 (5 ng)–injected control oocytes. THT1 is the *T. brucei* hexose transporter. There was no significant difference in $^{65}Zn^{2+}$ uptake between water- and THT1-injected groups ($P = 0.5$). (C) 2-DOG uptake in Mramp- (5 ng), THT1- (5 ng), and water-injected oocytes. THT1 induces significantly greater 2-DOG uptake than either Mramp ($P < 0.002$) or water ($P < 0.002$). There was no significant difference in uptakes between the water- and Mramp-injected oocytes. Displayed are mean values (± SE) of uptakes (10 oocytes per experimental condition).

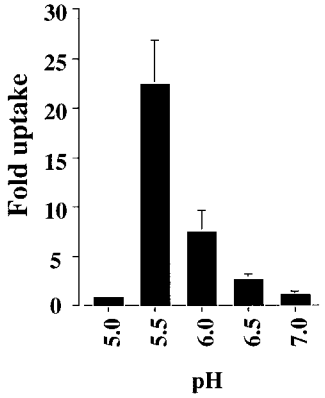

Figure 3. pH dependence of $^{65}Zn^{2+}$ uptake induced by Mramp. $^{65}Zn^{2+}$ uptake was assayed in Mramp-injected and control oocytes in media varying in pH (see Materials and Methods). The increase in $^{65}Zn^{2+}$ uptake (Fold) is shown for Mramp-expressing oocytes compared with controls. Uptakes at pH 5.5 ($P < 0.001$) and pH 6.0 ($P \leq 0.009$) were significantly greater than uptakes under remaining conditions. There were no significant differences in uptake at pH 5.0, 6.5, and 7.0 ($P > 0.1$). Displayed are mean values (± SE) of uptakes (10 oocytes per experimental condition).

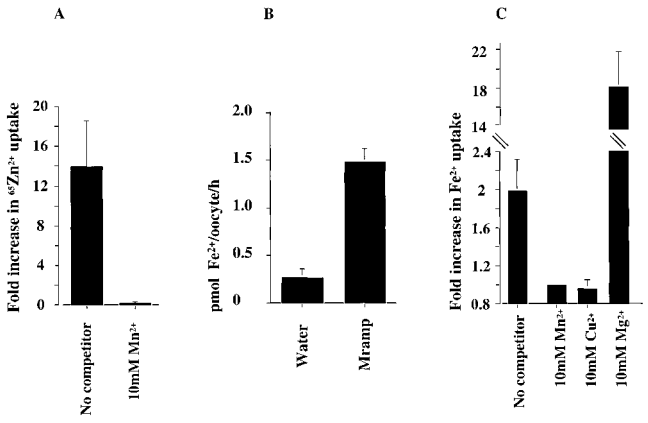

Figure 4. Substrate specificity for Mramp. (A) Abolition of $^{65}Zn^{2+}$ uptake by Mn^{2+} in Mramp RNA–injected oocytes. Increase in uptake compared with control oocytes in the absence and presence of Mn^{2+} (10 mM as $MnCl_2$; $P = 0.01$). (B) Uptake of $^{55}Fe^{2+}$ by Mramp RNA–injected oocytes compared with water-injected controls ($P < 0.001$). (C) Influence of divalent cation competitors on $^{55}Fe^{2+}$ (100 μM) uptake by *Mramp* RNA–injected oocytes. Data from one experiment. Displayed are mean values (± SE) of uptakes (10 oocytes per experimental condition).

compared with water-injected (Fig. 2 A) or *Mramp* antisense–injected controls (Fig. 2 A, inset). To confirm that these induced $^{65}Zn^{2+}$ uptakes were specific to *Mramp*, we also examined the uptake of $^{65}Zn^{2+}$ in oocytes injected with RNA made from the *Trypanosoma brucei* hexose transporter (THT1 [33]; Fig. 2 B). As expected, there was no increase in $^{65}Zn^{2+}$ uptake associated with expression of THT1, confirming the requirement for Mramp to induce $^{65}Zn^{2+}$ uptake. Conversely, we demonstrated 2′-deoxy-d[^{14}C]-glucose (2-DOG) uptake by THT1 but not by Mramp (Fig. 2 C). To confirm that accumulation of $^{65}Zn^{2+}$ continued beyond these experimental time points, we monitored $^{65}Zn^{2+}$ uptake for up to 4 h. The increase in uptake of $^{65}Zn^{2+}$ was linear during this period, which encompasses the uptake times of experiments shown (slope 3.8 ± 0.63, $P < 0.001$).

Mramp-induced $^{65}Zn^{2+}$ Uptake Is pH Dependent. In oocytes, translocation of divalent cations by DCT1 (the rat Nramp2 homologue) depends on cotransport of protons, with maximal activity of DCT1 at an extraoocytic pH of 5.5. To determine if cation transport by Mramp displays a similar pH dependence, we measured $^{65}Zn^{2+}$ uptake by oocytes incubated in extracellular pH values between 5.0 and 7.0. In nine independent experiments, $^{65}Zn^{2+}$ uptake by oocytes was confined to extracellular pH values between 5.5 and 6.5 (Fig. 3) and was completely abolished at pH 7 or 5.

Mramp Has Broad Cation Transport Specificity. As a first step to determine the specificity of Mramp for divalent cations in the *d*-block series, we measured the uptake of $^{65}Zn^{2+}$ in the presence of an excess of unlabeled Mn^{2+}. Mn^{2+} (10 mM) completely abolished uptake of $^{65}Zn^{2+}$ (Fig. 4 A), indicating that Mn^{2+} competes with $^{65}Zn^{2+}$ for binding to or uptake by Mramp.

We next used $^{55}Fe^{2+}$ as a permeant to investigate in detail the substrate specificity of Mramp for divalent cations. Mramp mediates large increases in the uptake of $^{55}Fe^{2+}$ at pH 5.5 (up to 18-fold) above water-injected oocytes (Fig. 4 B). This induced $^{55}Fe^{2+}$ uptake is abolished by Mn^{2+} and Cu^{2+} (Fig. 4 C). In contrast, Mg^{2+}, a divalent cation that does not belong to the *d*-block series, enhanced $^{55}Fe^{2+}$ accumulation by oocytes ninefold compared with $^{55}Fe^{2+}$ uptake in its absence (Fig. 4 C).

Mramp and y39 Expression Are Modulated by Changes in Ambient Iron and Copper Concentrations. Mycobacterial growth varied in media containing different concentrations of Fe^{2+} and Cu^{2+}. At relatively high concentrations (>45 μM), Fe^{2+} and Cu^{2+} inhibited bacterial growth by 29 and 38%, respectively (Fig. 5 B). *Mramp* mRNA transcript was detectable in bacteria grown at all Fe^{2+} and Cu^{2+} concentrations tested (Fig. 5 A), including a faint band in bacteria grown in Fe^{2+}-depleted culture medium, which was quantifiable using the GDS 7600 system but is not visible on the photograph. mRNA for *y39* was similarly detectable at all Fe^{2+} and Cu^{2+} concentrations. In contrast, mRNA for *yhho* gave much fainter bands in bacteria grown in high Fe^{2+} concentrations and medium and high Cu^{2+} concentrations, and was undetectable in other conditions. rRNA (16S) RT-PCR analysis of these templates confirmed that initial total RNA template quantities were comparable for all conditions (Fig. 5 A, bottom).

Semiquantitative analysis of PCR products from *Mramp* and *y39* (a putative Ca^{2+}-translocating P-type ATPase [17]) using identical template concentrations and PCR conditions showed large increases in mRNA for *Mramp* (~50-fold) as Fe^{2+} concentration increases from <1 to 48 μM (Fig. 5 A). As Cu^{2+} concentrations increase over a similar range, mRNA for *Mramp* increases ~10-fold, and is maximal at 5 μM Cu^{2+}. There is less increase in mRNA for *y39* under these conditions (~17- and 5-fold, respectively).

To investigate the regulation of *Mramp* and *y39* transcription more precisely, we used a ratiometric PCR technique called TC-PCR to quantitate mRNA for *Mramp* in relation to *y39* in *M. tuberculosis* cultured in media containing these different concentrations of Fe^{2+} and Cu^{2+}. The mRNA ratios for *Mramp*/*y39* fell fourfold (from 0.44 to 0.11) when Cu^{2+} concentrations increased from 5 to 70

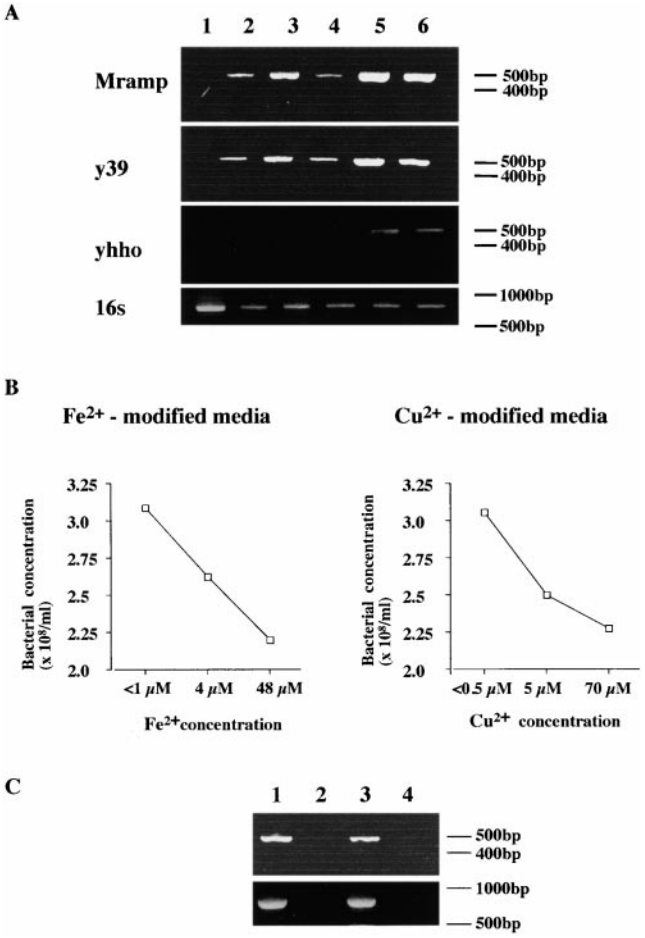

Figure 5. Growth of *M. tuberculosis* H37Rv in different cationic conditions. (A) RT-PCR for *Mramp* and *y39* carried out on total RNA isolated from *M. tuberculosis* H37Rv cultured in media containing different Fe^{2+} and Cu^{2+} concentrations. Equal amounts of RNA template (30 ng) were used in each reaction (3 ng for 16S RNA experiments). Lane 1, low Fe^{2+}(<1 μM); lane 2, medium Fe^{2+} (4 μM); lane 3, high Fe^{2+} (48 μM); lane 4, low Cu^{2+} (<0.5 μM); lane 5, medium Cu^{2+} (5 μM); lane 6, high Cu^{2+} (70 μM). (B) Bacterial growth after 5 wk culture at each metal ion concentration. (C) Top panel, RT-PCR for *Mramp* on total RNA isolated from axenically cultured and intracellular BCG. Equal amounts of RNA template (135 ng) were used in each reaction. Lane 1, template from extracellular (axenically cultured) BCG; lane 2, template from extracellular BCG pretreated with RNAse A; lane 3, template from intracellular BCG; lane 4, template from intracellular BCG pretreated with RNAse A. Bottom panel, RT-PCR for rRNA (16S) using amounts of total RNA template identical to top panel. Lane 1, template from extracellular (axenically cultured) BCG; lane 2, template from extracellular BCG pretreated with RNAse A; lane 3, template from intracellular BCG; lane 4, template from intracellular BCG pretreated with RNAse A.

μM. The relatively low PCR yields of product from *y39* except for bacteria grown in medium and high Cu^{2+} concentrations precluded more accurate quantitation of *Mramp*/*y39* mRNA ratios in these conditions.

Mramp Is Expressed by BCG in the Intracellular Environment. Fig. 5 C (top) shows that mRNA encoding Mramp is detectable in RNA extracted from intracellular BCG. For comparison, we show that *Mramp* mRNA is also detectable in axenically cultured BCG under identical PCR conditions. Comparability of template concentrations in this experiment was verified by RT-PCR analysis of rRNA (16S) (Fig. 5 C, bottom).

Discussion

Although approximately 1.7 billion people (one third of the world's population) are infected with *M. tuberculosis* at any one time, it is striking that, in the absence of coinfection with HIV, fewer than 10% of these will develop active disease during their lifetimes (34). Host genetic factors such as polymorphisms in *Nramp1* clearly influence susceptibility to infection or disease caused by *Mycobacteria* species (35). For example, tuberculosis in a tribally mixed Gambian population was associated with two pairs of *Nramp1* polymorphisms (8), and in another study involving members of Chinese and Vietnamese families with leprosy, haplotypes associated with *Nramp1*-linked polymorphisms were observed to be distributed nonrandomly between affected and unaffected family members (9).

The Nramp family of proteins is highly conserved between bacteria and mammals, and two eukaryotic examples have been shown to transport divalent cations such as Fe^{2+} and Mn^{2+} (12, 36, 37). Nramp1 is likely to perform similar transport functions to Nramp2, which mediates pH-dependent Fe^{2+} uptake in heterologous expression studies and in vivo (12, 36). Defining the transport specificities for Nramp1 has proved difficult (38), and all studies characterizing Nramp homologues have been carried out exclusively on eukaryotic sequences. Recent studies in RAW264.7 cells overexpressing Nramp1 suggest that Nramp1 does contribute to iron mobilization from vesicles (39). Nramp1 also circumvents maturation arrest of phagosomes containing live BCG, permitting the increase in acidification normally seen in phagosomes containing killed BCG or latex beads (40). These observations point to the possibility that competition for transition metal ions may be important in determining maturational dynamics of phagosomes as well as their lethality for certain intracellular pathogens.

We studied a mycobacterial homologue of the Nramp family because of its potential relevance to intracellular survival. Nramp homologues are found in *M. tuberculosis*, *M. leprae*, *M. smegmatis*, and BCG (7, 17). These homologues (called Mramp) have been suggested to mediate the uptake of cations such as Fe^{2+}, Mn^{2+}, and Zn^{2+}, which may be important in defence by microbial superoxide dismutase against the macrophage respiratory burst (17, 18). Our studies now provide direct evidence for a function of Mramp as a transporter of Zn^{2+} and Fe^{2+}.

Furthermore, the enhanced uptake of $^{65}Zn^{2+}$ and $^{55}Fe^{2+}$ induced in oocytes expressing Mramp is abrogated by an excess of Mn^{2+} and Cu^{2+}, but not by unrelated divalent cations such as Mg^{2+}, suggesting important interactions between Mramp and these transition elements. In spite of divergence in primary sequence between Nramp1, DCT1 (a rat intestinal homologue of Nramp2), and Mramp and their diverse phylogeny, all three sequences can mediate the uptake of Fe^{2+} into *Xenopus* oocytes (12). DCT1 transports other members of the transition metal series, and this broad

specificity is also observed for Mramp. Therefore, Mramp represents a novel class of prokaryotic metal ion transporter with representatives in other bacteria such as *E. coli* and *B. subtilis* (Fig. 1).

We examined the pH dependence of cation transport by Mramp using $^{65}Zn^{2+}$ as a permeant, because at pH $>$ 6.0 it is difficult to manipulate the equilibrium between Fe^{2+} and Fe^{3+} even in the presence of reducing agents such as ascorbic acid (41). There is a narrow range of extracellular acid pH values that allows Mramp-induced uptake of $^{65}Zn^{2+}$ by oocytes. This pH range (5.5–6.5) coincides with estimates of ambient pH in the microenvironment of intraphagosomal mycobacteria (42). This observation also provides evidence for the direction in which cation transport is likely to be taking place, namely from the relatively acidic phagosome into mycobacteria. By contrast, an uninfected phagolysosome (for example, one containing inert particles) has a significantly lower pH ($<$5.5 [42]), and would therefore be unlikely to allow efficient transport of divalent cations by Mramp.

To assess the expression of *Mramp* in *M. tuberculosis* cultured axenically, we applied a precise assay to quantitate mRNA for *Mramp* obtained from organisms grown in media containing defined Cu^{2+} and Fe^{2+} concentrations. These studies permitted assessment of the growth characteristics of bacteria as well as the relative expression of mRNA for Mramp compared with mRNA encoding a putative Ca^{2+} P-type ATPase (y39). Mramp is expressed poorly in bacteria grown in relatively Cu^{2+}- and Fe^{2+}-deficient media, and expression is enhanced at higher concentrations of these metal ions ($\geq$5 μM). Similar patterns of mRNA expression are observed for the putative Ca^{2+}-transporting P-type ATPase (y39), but in contrast, mRNA encoding an atypical heavy metal-translocating P-type ATPase (yhho) is barely detectable under any of the conditions tested (Fig. 5). This stimulation of expression of mRNA for *Mramp* and *y39* at higher ambient concentrations of $Cu^{2+}$and Fe^{2+} is associated with retardation of bacterial growth by $\sim$30%.

mRNA for *Mramp* encoded by BCG is clearly expressed in the intracellular environment (Fig. 5 C). We used BCG as a model for *M. tuberculosis* because *M. tuberculosis* is frequently cytopathic when cultured in THP1 cells, compromising yields of RNA. BCG is well recognized as a convenient model to study mycobacterial gene expression in these circumstances (25).

Mramp may act in concert with mechanisms inhibiting acidification of phagosomes to permit intracellular survival of mycobacteria. The deployment of Nramp1 in the host's phagosomal membrane is clearly important in defence against infection, as established by classical studies on the genetics of Nramp1. If Nramp1 also uses phagosomal protons to extrude cations, thereby competing with Mramp, the pH dependence of this phenomenon will be critical in establishing which of the two transporters (Mramp or Nramp1) functions most efficiently in the infected macrophage. Experiments to examine this hypothesis in greater detail can now be formulated on the basis of Mramp's function as defined by heterologous expression. Mramp is the first mycobacterial gene to be expressed in oocytes, exemplifying the utility of this system for the functional characterization of other prokaryotic transporters (*E. coli* glycerol facilitator glpF, and *E. coli* water channel AqpZ [43]).

We thank Dr. T. Balz for the THT1 clone, and Dr. G. Gould for the pSPGT1 clone.

D. Agranoff is a Medical Research Council Training Fellow, and S. Krishna is a Wellcome Trust Senior Research Fellow in Clinical Science. I.M. Monahan, J.A. Mangan, and P.D. Butcher acknowledge the support of the European Union and Medical Research Council (UK), and J.A. Mangan, P.D. Butcher, and S. Krishna acknowledge Medical Research Council Co-operative Grant G9800300 for support.

Address correspondence to Sanjeev Krishna, Department of Infectious Diseases, St. George's Hospital Medical School, Cranmer Terrace, London SW20 ORE, UK. Phone: 181-725-5836; Fax: 181-725-3487; E-mail: s.krishna@sghms.ac.uk

Submitted: 31 March 1999 Revised: 2 June 1999 Accepted: 6 July 1999

References

1. Sinai, A.P., and K.A. Joiner. 1997. Safe haven: the cell biology of nonfusogenic pathogen vacuoles. *Annu. Rev. Microbiol.* 51:415–462.
2. Russell, D.G. 1992. *Mycobacterium* and *Leishmania*: stowaways in the endosomal network. *Trends Cell Biol.* 5:126–129.
3. Vidal, S., P. Gros, and E. Skamene. 1995. Natural resistance to infection with intracellular parasites: molecular genetics identifies *Nramp1* as the *Bcg/Ity/Lsh* locus. *J. Leukocyte Biol.* 58:382–390.
4. Cellier, M., A. Belouchi, and P. Gros. 1996. Resistance to intracellular infections: comparative genomic analysis of *Nramp*. *Trends Genet.* 12:201–204.
5. Plant, J., and A.A. Glynn. 1976. Genetics of resistance to infection with *Salmonella typhimurium* in mice. *J. Infect. Dis.* 133:72–78.
6. Bradley, D.J. 1977. Regulation of *Leishmania* populations within the host. II. Genetic control of acute susceptibility of mice to *Leishmania donovani* infection. *Clin. Exp. Immunol.* 30:130–140.
7. Skamene, E., P. Gros, A. Forget, P.A.L. Kongshavn, C. St. Charles, and B.A. Taylor. 1982. Genetic regulation of resistance to intracellular pathogens. *Nature.* 297:506–509.
8. Bellamy, R., C. Ruwende, T. Corrah, K.P.W.J. McAdam, H.C. Whittle, and A.V.S. Hill. 1998. Variations in the *NRAMP1* gene and susceptibility to tuberculosis in West African patients. *N. Engl. J. Med.* 338:640–644.

9. Abel, L., F.O. Sánchez, J. Oberti, N.V. Thuc, L.V. Hoa, V.D. Lap, E. Skamene, P.H. Lagrange, and E. Schurr. 1998. Susceptibility to leprosy is linked to human *NRAMP1* gene. *J. Infect. Dis.* 177:133–145.
10. Pinner, E., S. Gruenheid, M. Raymond, and P. Gros. 1997. Functional complementation of the yeast divalent cation transporter family *SMF* by *NRAMP2*, a member of the mammalian natural resistance-associated macrophage protein family. *J. Biol. Chem.* 272:28933–28938.
11. Fleming, M.D., M.A. Romano, M.A. Su, L.M. Garrick, M.D. Garrick, and N.C. Andrews. 1998. *Nramp2* is mutated in the anemic Belgrade (*b*) rat: evidence of a role for Nramp2 in endosomal iron transport. *Proc. Natl. Acad. Sci. USA*. 95: 1148–1153.
12. Gunshin, H., B. MacKenzie, U.V. Berger, Y. Gunshin, B. Romero, W.F. Boron, S. Nussberger, J.L. Gollan, and M.A. Hediger. 1997. Cloning and characterization of a mammalian proton-coupled metal-ion transporter. *Nature*. 388:482–488.
13. Orgad, S., H. Nelson, D. Segal, and N. Nelson. 1998. Metal ions suppress the abnormal taste behavior of the *Drosophila* mutant *malvolio*. *J. Exp. Biol.* 201:115–120.
14. Gruenheid, S., E. Pinner, M. Desjardins, and P. Gros. 1997. Natural resistance to infection with intracellular pathogens: the *Nramp1* protein is recruited to the membrane of the phagosome. *J. Exp. Med.* 185:717–730.
15. Fridovich, I. 1989. Superoxide dismutases. *J. Biol. Chem.* 264:7761–7764.
16. Zhang, Y., R. Lathigra, T. Garbe, D. Catty, and D. Young. 1991. Genetic analysis of superoxide dismutase, the 23 kilodalton antigen of *Mycobacterium tuberculosis*. *Mol. Microbiol.* 5:381–391.
17. Agranoff, D., and S. Krishna. 1998. Metal ion homeostasis and intracellular parasitism. *Mol. Microbiol.* 28:403–412.
18. Supek, F., L. Supekova, H. Nelson, and N. Nelson. 1997. Function of metal-ion homeostasis on the cell division cycle, mitochondrial protein processing, sensitivity to mycobacterial infection and brain function. *J. Exp. Biol.* 200:321–330.
19. Skamene, E., E. Schurr, and P. Gros. 1998. Infection genomics: *Nramp1* as a major determinant of natural resistance to intracellular infections. *Annu. Rev. Med.* 49:275–287.
20. Altshul, S.F., T.L. Madden, A.A. Schäffer, J. Zhang, Z. Zheng, U. Miller, and D.J. Lipman. 1997. Gapped BLAST and PSI-BLAST: a new generation of protein database search programs. *Nucleic Acids Res.* 25:3389–3402.
21. Gould, G., and G.E. Lienhard. 1989. Expression of a functional glucose transporter in *Xenopus* oocytes. *Biochemistry*. 28:9447–9452.
22. Penny, J.I., S.T. Hall, C.J. Woodrow, G. Cowan, A.M. Gero, and S. Krishna. 1998. Expression of substrate-specific transporters by *Plasmodium falciparum* in *Xenopus laevis* oocytes. *Mol. Biochem. Parasitol.* 93:81–89.
23. Colman, A. 1984. Translation of eucaryotic messenger RNA in *Xenopus* oocytes. *In* Transcription and Translation - A Practical Approach. 1st. ed. B.D. Hames and S.J. Higgins, editors. IRL Press, Oxford. 271–302.
24. Fish, W.W. 1988. Rapid colorimetric micromethod for the quantitation of complexed iron in biological samples. *Methods Enzymol.* 158:357–364.
25. Butcher, P.D., J.A. Mangan, and I.M. Monahan. 1998. Intracellular gene expression. *In* Methods in Molecular Biology, 1st ed. Mycobacteria Protocols, Vol. 101. T. Parish and N.G. Stoker, editors. Humana Press, Inc., Totowa, NJ. 472.
26. Mangan, J.A., K.M. Sole, D.A. Mitchison, and P.D. Butcher. 1997. An effective method of RNA extraction from bacteria refractory to disruption, including mycobacteria. *Nucleic Acids Res.* 25:675–676.
27. Virdi, A.S., S. Krishna, and B.C. Sykes. 1992. Tandem competitive polymerase chain reaction (TC-PCR): a method for determining ratios of RNA and DNA templates. *Mol. Cell. Probes*. 6:375–380.
28. Kim, J., M. Puder, and R.J. Soberman. 1996. Joining of DNA fragments by repeated cycles of denaturation, annealing and extension. *Biotechniques*. 6:954–955.
29. Woodrow, C.J., J. Penny, and S. Krishna. 1999. Intraerythrocytic *Plasmodium falciparum* expresses a high-affinity facilitative hexose transporter. *J. Biol. Chem.* 274:7272–7277.
30. Cole, S.T., R. Brosch, J. Parkhill, T. Garnier, C. Churcher, D. Harris, S.V. Gordon, K. Eiglmeier, S. Gas, C.E. Barry III, et al. 1998. Deciphering the biology of *Mycobacterium tuberculosis* from the complete genome sequence [published erratum appears in *Nature*. 1998. 396:190]. *Nature*. 393:537–544.
31. Cellier, M., G. Privé, A. Belouchi, T. Kwan, V. Rodrigues, W. Chia, and P. Gros. 1995. Nramp defines a family of membrane proteins. *Proc. Natl. Acad. Sci. USA*. 92:10089–10093.
32. von Heijne, G. 1994. Membrane proteins: from sequence to structure. *Annu. Rev. Biophys. Biomol. Struct.* 23:167–192.
33. Bringaud, F., and T. Baltz. 1992. A potential hexose transporter gene expressed predominantly in the bloodstream form of *Trypanosoma brucei*. *Mol. Biochem. Parasitol.* 52:111–122.
34. Bloom, B.R., editor. 1994. Tuberculosis. Pathogenesis, Protection and Control. ASM Press, Washington, DC. 500 pp.
35. Hill, A.V.S. 1998. Immunogenetics of human infectious diseases. *Annu. Rev. Immunol.* 16:593–617.
36. Fleming, M.D., C.C. Trenor III, M.A. Su, D. Foernzler, D.R. Beier, W.F. Dietrich, and N.C. Andrews. 1997. Microcytic anaemia mice have a mutation in *Nramp2*, a candidate iron transporter gene. *Nat. Genet.* 16:383–386.
37. Supek, F., L. Supekova, H. Nelson, and N. Nelson. 1996. A yeast manganese transporter related to the macrophage protein involved in conferring resistance to mycobacteria. *Proc. Natl. Acad. Sci. USA*. 93:5105–5110.
38. Govoni, G., and P. Gros. 1998. Macrophage NRAMP1 and its role in resistance to microbial infections. *Inflamm. Res.* 47: 277–284.
39. Atkinson, P.G., and C.H. Barton. 1999. High level expression of Nramp1G169 in RAW264.7 cell transfectants: analysis of intracellular iron transport. *Immunology*. 96:656–662.
40. Hackam, D.J., O.D. Rotstein, W.-j. Zhang, S. Gruenheid, P. Gros, and S. Grinstein. 1998. Host resistance to intracellular infection: mutation of natural resistance–associated macrophage protein 1 (*Nramp1*) impairs phagosomal acidification. *J. Exp. Med.* 188:351–364.
41. Dorey, C., C. Cooper, D.P.E. Dickson, H.F. Gibson, R.J. Simpson, and Y.J. Peters. 1993. Iron speciation at physiological pH in media containing ascorbate and oxygen. *Br. J. Nutr.* 70:157–169.
42. Sturgill-Koszycki, S., P.H. Schlesinger, P. Chakraborty, P.L. Haddix, H.L. Collins, A.K. Fok, R.D. Allen, S.L. Gluck, J. Heuser, and D.G. Russell. 1994. Lack of acidification in *Mycobacterium* phagosomes produced by exclusion of the vesicular proton-ATPase. *Science*. 263:678–681.
43. Maurel, C., J. Reizer, J.I. Schroeder, M.J. Chrispeels, and M.H. Saier, Jr. 1994. Functional characterization of the *Escherichia coli* glycerol facilitator, GlpF, in *Xenopus* oocytes. *J. Biol. Chem.* 269:11869–11872.